"Static Structural Analysis and Crack Propagation Analysis of Thermoplastic Poly Olefin (TPO) Based Car (TATA Indigo) Rear Bumper Right Side Protector using ANSYS 13.0 With It's Original Material and Two other Optimized Materials(PP+EOC+ATP, PP+EPDM)"

Ipsa Mohapatra
Department of Mechanical Engineering,
D.Y. Patil College of Engineering
Akurdi, Pune 411044, Maharashtra, India

Sushovit Mohanty
Finolex Industries Limited
Pune 411057, Maharashtra, India

Abstract: **- The main purpose of this research is to analyse the overall structural stability of the chosen product from application point of view through Finite Element Analysis (FEA) technique using ANSYS13 Workbench. Then Crack propagation analysis to verify it's work life by providing notches of different radii using the same above technique. To track the crack propagation a different method using a deformation probe at the tip of the notch is suggested. To perform all the experiments three different materials, one is the original material of the product itself and two other optimized materials PP+EOC+ATP, PP+EPDM is used. Then compare all the results obtained and analyse different results with reference to its original material. Thus a comparative study can suggest the most suitable material for the product.**

Key words: Finite Element Analysis, ANSYS13 Workbench, Crack Propagation, Notch, Deformation probe, PP+EOC+ATP, PP+EPDM.

I. INTRODUCTION

Failure of the engineering structures is caused by cracks, which is depending on the design and operating conditions that extend beyond a safe size. Cracks present to some extent in all structures, either as a result of manufacturing defects or localized damage in service. The crack growth leads to a decrease in the structural strength. Thus, when the service leading to the failure of the structure. Fracture, the final catastrophic event takes place very rapidly and is preceded by crack growth, which develops slowly during normal service conditions.

It is of particular interest to investigate the structure-property of rubber-rich TPO blends reinforced with rigid nanofillers. The effect of nanoclay additions on the structure and property of rubber-rich TPO blends has been investigated by Mishra et al. [1] and Tjong and Ruan [1] more recently. Mishra et al. [1] prepared the TPO/clay nanocomposites where the TPO contains PP and EPDM with the ratio of 25 : 100 by weight. They reported that the nanocomposites exhibit remarkable improvement of tensile and storage modulus over their pristine TPO blends. Tjong and Ruan [2] reported that TPO-based nanocomposites reinforced with 0.1–1.5wt% organically modified clay exhibits enhanced stiffness and tensile strength. Moreover, the fracture toughness of TPO/clay nanocompsites increases with the increasing clay content.

Ananda Kumar Eriki and Ravichandra R have already investigated the Spur Gear Crack Propagation Path Analysis Using Finite Element Method [6]. Mubashir Gulzar has studied Linear and Non Linear Analysis of Central Crack Propagation in Polyurethane Material [7]. Priscilla L. Chin has studied Stress Analysis, Crack Propagation and Stress Intensity Factor Computation of a Ti-6Al-4V Aerospace Bracket using ANSYS and FRANC3D [8].

Here in this thesis the crack propagation path has been studied through a different technique. In this technique a special element called a deformation probe is placed over the crack tip, which will create the stress singularity at the crack tip [3]. Then for different loadings the propagation of the crack tip is being measured in any of the X, Y and Z directions. The entire analysis is carried out in ANSYS13 using a set of boundary and loading conditions.

II. EXPERIMENTAL DETAILS

A. Finite element model:

1). Geometric model: First step in all numerical analysis methods is to develop a finite element (FE) model which includes geometry, set of assumptions and loading conditions used to define the real physical problem. Modelling is an unambiguous representation of the parts of an object which is suitable for computer processing. The model for the FEA is created with all the actual dimensions using CATIA-V5 . CATIA-V5 is a parametric, feature-based solid modelling system. The main features of the geometric model of the Protector are demonstrated in Figure 1.1. The detailed engineering drawing of the protector including the dimension of all the parts is provided in Figure 1.2.

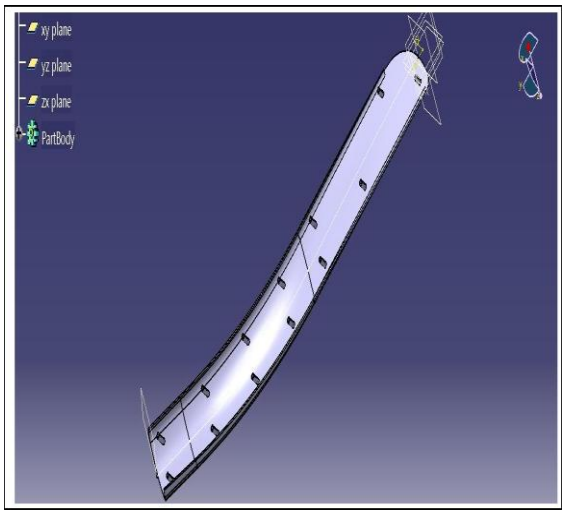

Figure 1.1 Redesigning of product model in CATIA-V5

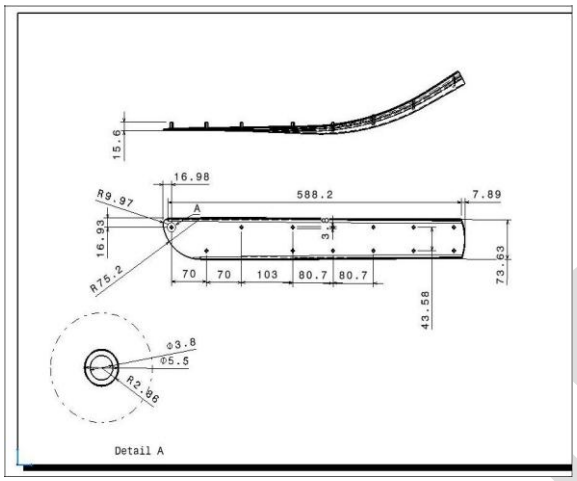

Figure 1.2 Drafting of the product model

2) Assumptions: In most of the cases it is not possible to develop a FE model that can exactly represent the real physical system particularly in the case of complex engineering systems. In order to develop a FE model which is close to the reality, the researchers have to consider all aspects of the problem which make the FE model complex and increase the computational time. In order to simplify the complex FE models the researcher relay on a certain set of assumptions. The assumptions used in this project are described as follows;

- A set of ramped load ranging from 500N to 4000N is applied for the Notched specimen.
- The load is applied on the product in positive X direction.
- All the 13 positions at the strain tensors are rigidly fixed.
- The entire product is considered as the RVE (Representative Volume Element) for the testing.
- The RVE is considered as the single solid body.
- The testing is carried out at normal atmospheric pressure and temperature.

3). Material Properties: The Protector structure is modelled by three different linear elastic isotropic materials which are given in the table with their properties. Because of the thin wall thickness of 1.5mm, the model is idealized by shell elements [24].

TABLE-1

Sl no	Name	Density (ρ)	Poisson's Ratio(μ)	Young's Modulus (E)	Tensile Yield Strength	Tensile Ultimate Strength
	Unit	gm/cm^3		MPa	MPa	MPa
1	Original Material	0.9198	0.226	177.98	10.538	10.538
2	PP+EOC+ATP	0.9243	0.1567	438.87267	23.941	23.941
3	PP+EPDM	0.90616	0.4	392.50975	20.424	20.424

4). Boundary conditions: During the operating conditions different types of loadings are acting on the Protector boundary. Because of the vibrant nature of the Protector it is very difficult to model such a product with actual operating conditions. For the analysis purpose, certain set of boundary conditions are defined. The purpose of these conditions is to simplify the model without losing a realistic approximation of the Protector. The set of boundary conditions that are used in this project are demonstrated in Figure 1.3. The detail description of these boundary conditions is given as follows;

- All the 13 strain tensor points are rigidly fixed with fixed supports so that displacements in all degrees of freedom (DOF) are fixed.
- Now the Protector can't have any relative motion as required as its real application.

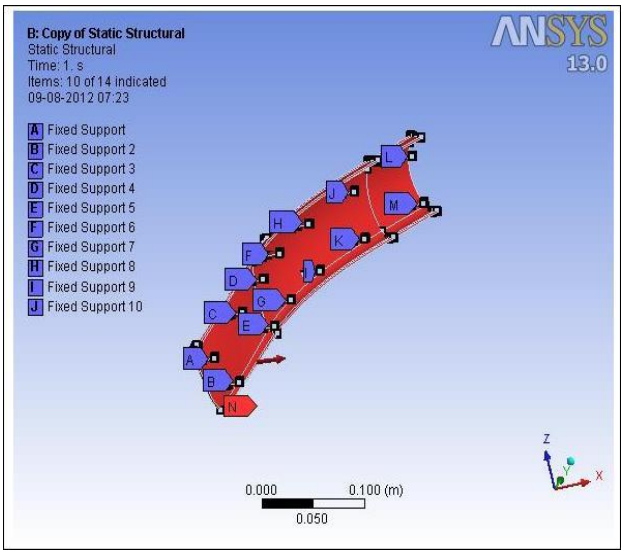

Figure 1.3 Boundary conditions used in the FE model

5). Loading conditions: The overall loading conditions are very complex because of the limitations to create the actual working conditions. In order to make a best approximation of the loading conditions, a complete research is conducted to determine an equivalent load that can be used instead of the real complex loading conditions. After several investigations it is concluded that the overall loadings can be replaced with an equivalent load ranging from 500N to 4000N in positive X direction along with a set of boundary conditions explained in section 2.1.4. Figure 1.4 demonstrate the loading condition used in this FE model.

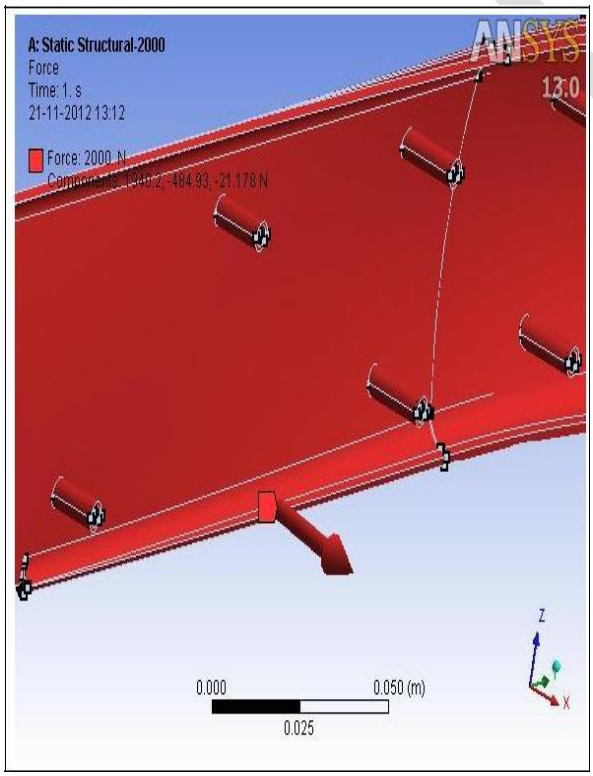

Figure 1.4: Loading conditions used in the FE model

B. Crack propagation analysis:

This chapter deals with the modelling techniques that are used to study the crack propagation analysis using ANSYS13. In this project the FE model for ANSYS13 is created in CATIA-V5 which is a kind of solid modelling software, however, it is also possible to have models generated from other programs with similar features. The initial model is a basic requirement in order to perform the simulations in ANSYS13.

1). Introduction: Computational techniques for evaluating fracture parameters, such as the SIF or crack propagation rate, requires either a refined mesh around the crack tip or the use of "special elements" which must possess the ability to incorporate the stress singularity near the crack tip.

2). FE model formulation:

a. Geometric model: First step in all numerical analysis methods is to develop a finite element (FE) model which includes geometry, set of assumptions and loading conditions used to define the real physical problem. Modelling is an unambiguous representation of the parts of an object which is suitable for computer processing. The model with Notches of different dimensions for the FEA is created with all the actual dimensions using CATIA-V5. CATIA-V5 is a parametric, feature-based solid modelling system. The main features of the geometric model of the Protector with Notches are demonstrated in Figure 1.5. The detailed engineering drawing of the protector including the dimension of all the parts is provided in Figure 1.6.

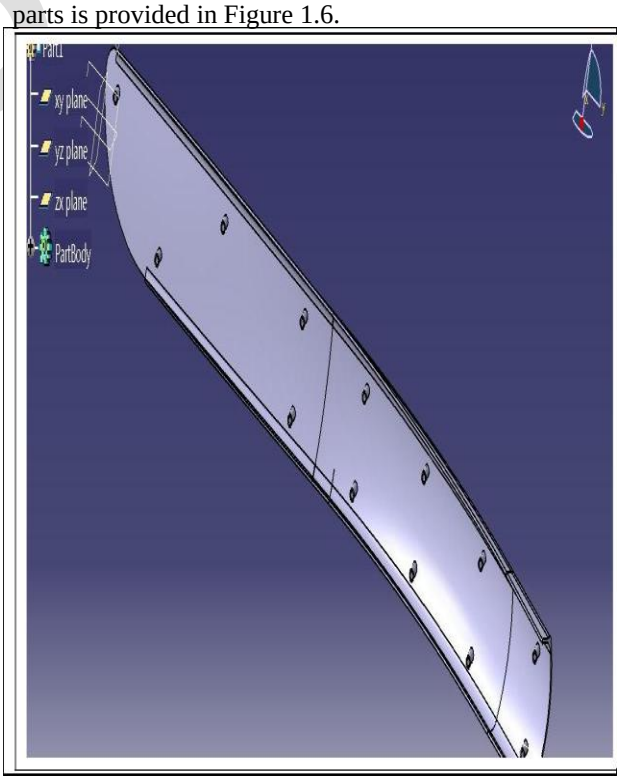

Figure 1.5 Redesigning of product model with a Notch in CATIA-V5

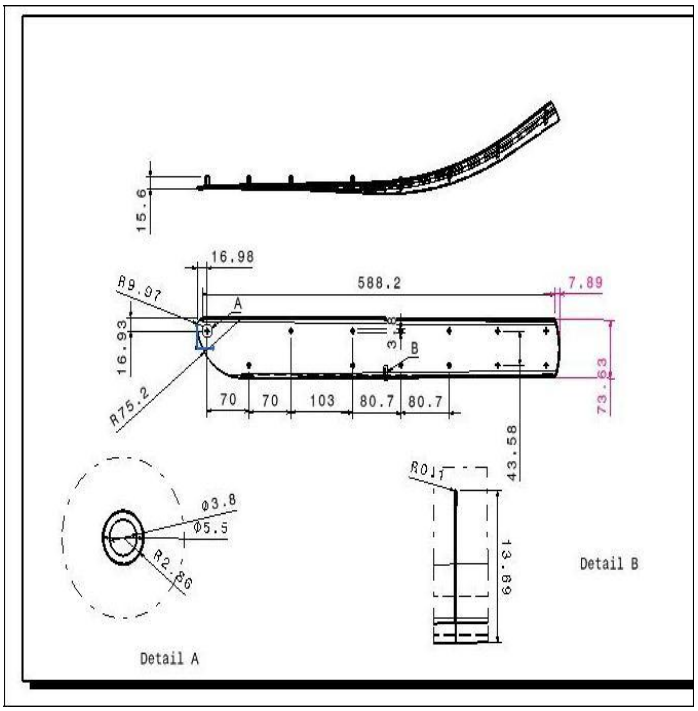

Figure 1.6 Drafting of the product model with a Notch

3). Notch Radius: The Notch is provided on the product to initiate the crack. Thus the radius of the Notch is having a critical impact on the propagation of the crack. So there are five different Notch radius is taken to judge it's impact on crack propagation. The radii taken are 0.1mm, 0.3mm, 0.5mm, 0.7mm, 0.9mm.

4). Local Coordinate System: To judge the crack propagation, it is needed to have a special element at the tip of the crack. So for that the tip of the crack is to be singularized and it is possible if the crack tip will be made as origin. Hence the tip of the crack is assigned as the origin of a Local coordinate system. The graphical arrangement of the Local coordinate system is shown in Figure 1.7 and the value of the coordinates of the origin of the local coordinate system is shown in Figure 1.8 as follows:

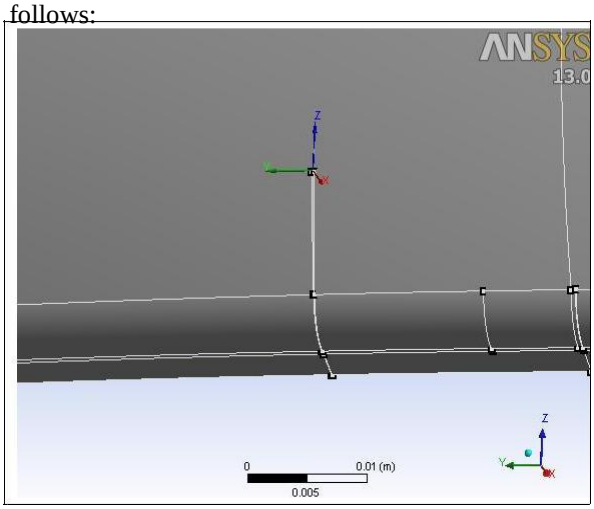

Figure 1.7 Local Coordinate System

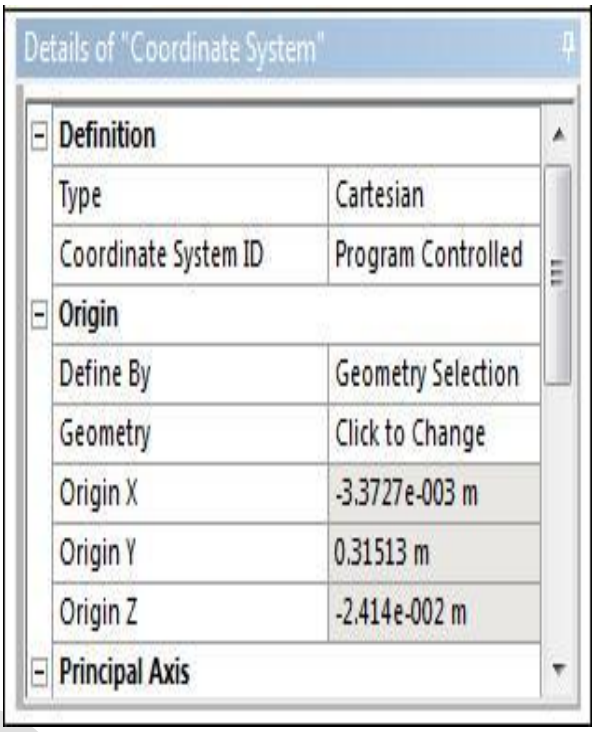

Figure 1.8 coordinates of the local Origin

5). Deformation Probe: To judge the crack propagation it will be suitable if we can have the displacement of the crack tip. For that the crack tip is provided with a special element called, a deformation probe on the origin of the local coordinate system. Now after every loading condition the displacement of the crack tip can be found out in any of the X, Y and Z directions. From that the crack propagation rate and direction both can be found out. The attachment of a deformation probe on the origin of the local coordinate system is shown in Figure 1.9 as follows:

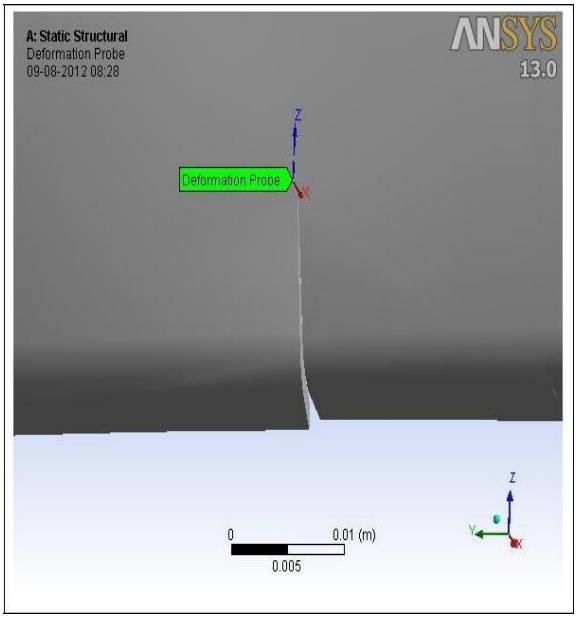

Figure 1.9 Positioning of Deformation probe

C. Finite Element Analysis:

In this chapter a brief summary of the different analysis approaches that have been used and the corresponding simulation results are presented. The main purpose of numerical simulations is to understand the shape deformation and stress distribution behaviour of the product, and to compare these results for the three different materials taken in the analysis. The FE model defined in this chapter is imported first into ANSYS [25] in order to perform the simulations and the results are obtained in the form of shape deformations and stress distribution.

1. Finite element model: The FE model defined in this chapter is imported into ANSYS with the same boundary conditions, loading conditions and material properties. The FE model is meshed in ANSYS using SHELL93 elements [26]. The SHELL93 elements are particularly well suited to model curved channel structures. The element has six DOF at each node; three translations and three rotations DOF. The deformation shapes are quadratic in both in-plane directions. The demonstration of SHELL93 elements is shown in figure 1.10.

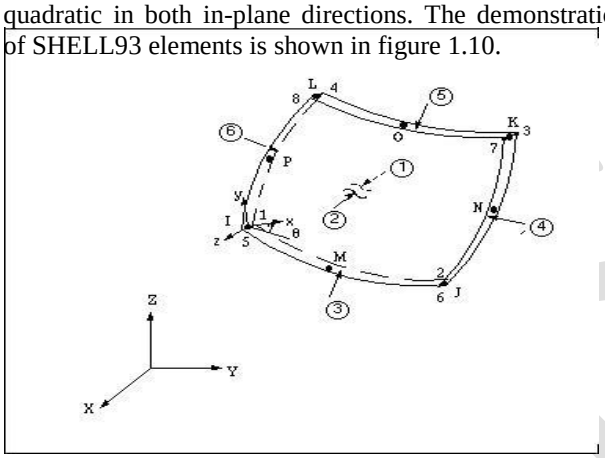

Figure 1.10: A SHELL93 element implemented in ANSYS

The thickness of the shell elements is a defined parameter and therefore do not have any elements in that direction. The computational savings come about because the mid-surface of the structure is modelled; the thickness and other cross-sectional properties are incorporated into the element stiffness matrix and input as "real constants" in ANSYS. The meshed product is shown in Figure 1.11.

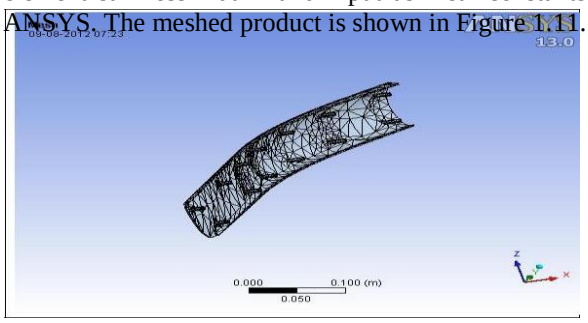

Figure 1.11: FE mesh of the Protector model in ANSYS

III. RESULT AND DISCUSSION

A. Simulation results for static structural Analysis:

After performing the simulation in ANSYS for a 2000N ramped load the results are obtained in the form of deformations and stress distributions. The results obtained from ANSYS are described as follows;

1. Deformation results: The deformation behaviours obtained from FE analysis for a 2000N ramped load are compared for the three reference materials. It has been found, that the structural deformation behaviour is non-symmetric. The values obtained are in good acceptable range and the maximum value is found to be 13.281mm for the original material as shown in figure 1.12 and the minimum value is found to be 6.7999mm for the material PP+EPDM.

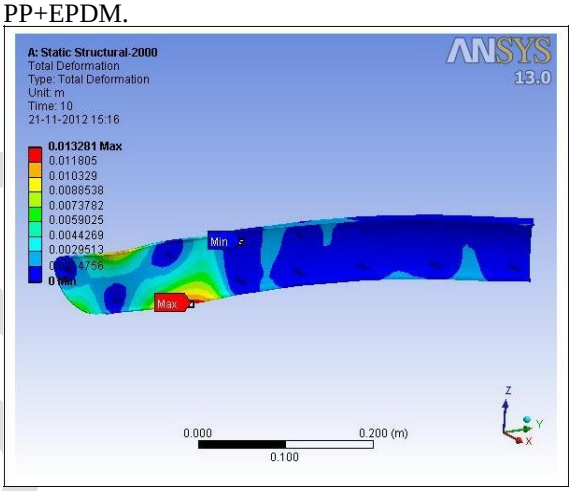

Figure 1.12 Deformation pattern – Original Material

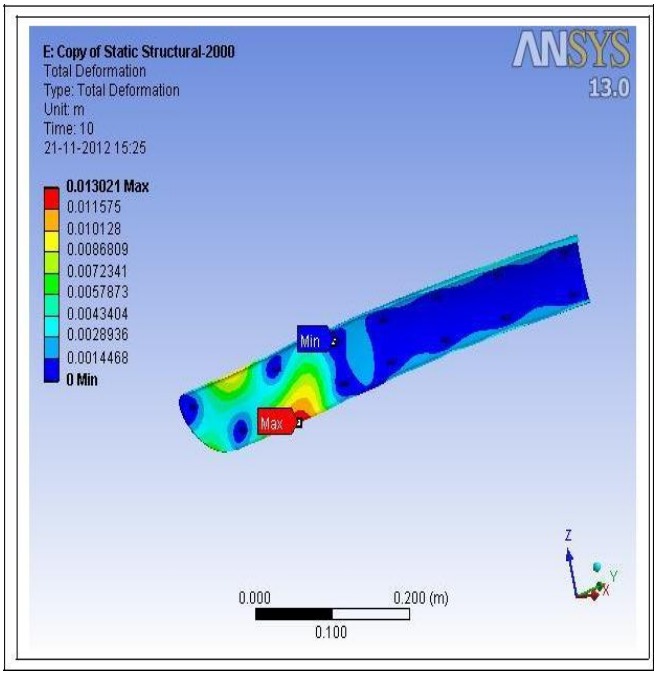

Figure 1.13 Deformation pattern – PP+EOC+ATP

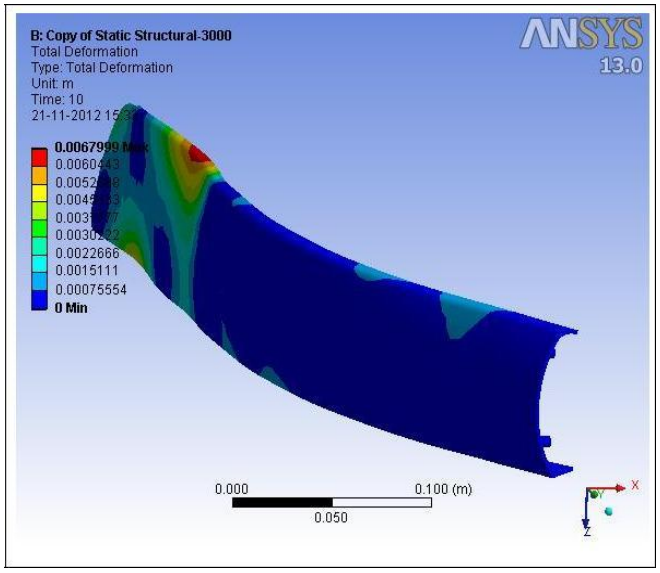

Figure 1.14 Deformation pattern – PP+EPDM

2. Stress distribution results: The stress distribution results are obtained in the form of Von-Misses stresses and a maximum value is found to be 30.696MPa for the material PP+EOC+ATP as shown in Figure 1.16 and a minimum value is found to be 11.046MPa for the material PP+EPDM. Like the deformation results, the stress distribution is also non-symmetric and the maximum stresses are found around the strain tensor. It has been observed that the stress distribution behaviour around each strain tensor is consistent. Figure 1.15, Figure 1.16 and Figure 1.17 demonstrate the location of the maximum Von Misses stress and the stress distribution behaviour around the strain tensor.

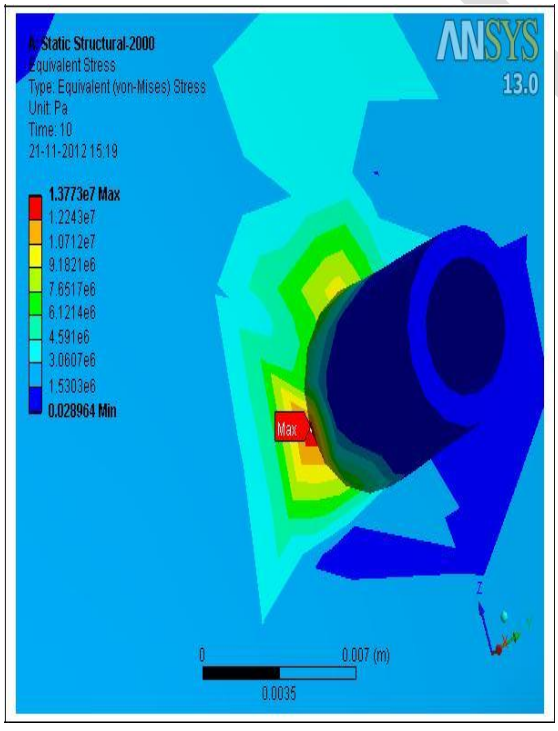

Figure 1.15: Von-Misses stress distribution – Original Material

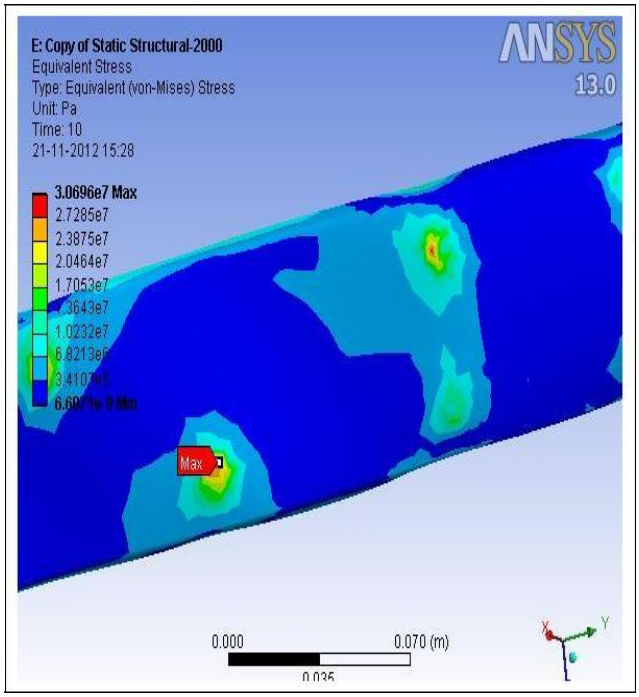

Figure 1.16: Von-Misses stress distribution – PP+EOC+ATP

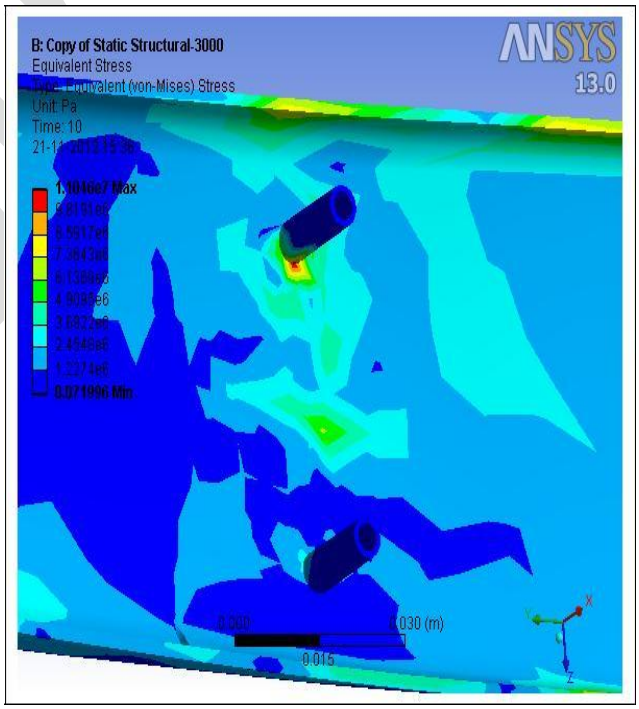

Figure 1.17: Von-Misses stress distribution – PP+EPDM

3. Strain distribution results: The strain distribution results are obtained in the form of Von-Misses strains and a maximum value is found to be 0.077386 for the Original material as shown in Figure 1.18 and a minimum value is found to be 0.028143 for the material PP+EPDM as shown in Figure 1.20. Like the stress distribution results, the strain distribution is also non-symmetric and the maximum strains are found around the strain tensor. It has been observed that the strain distribution behaviour around each strain tensor is consistent. Figure 1.18, Figure

1.19 and Figure 1.20 demonstrate the location of the maximum Von Misses strain and the strain distribution behaviour around the strain tensor.

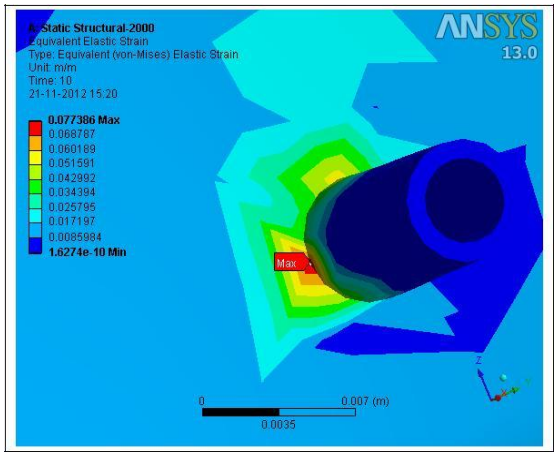

Figure 1.18: Von-Misses strain distribution – Original Material

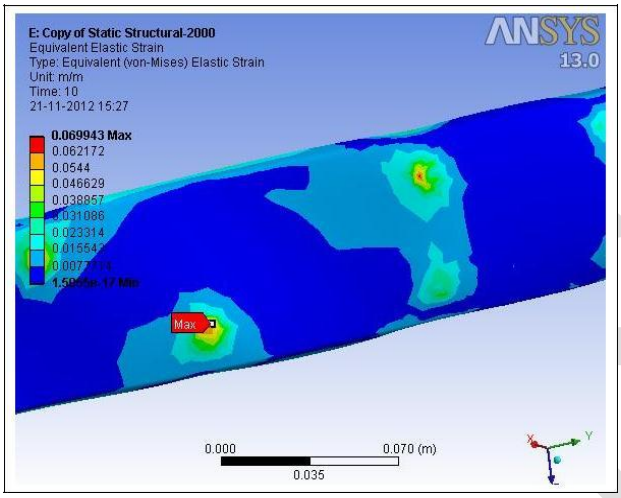

Figure 1.19: Von-Misses strain distribution – PP+EOC+ATP

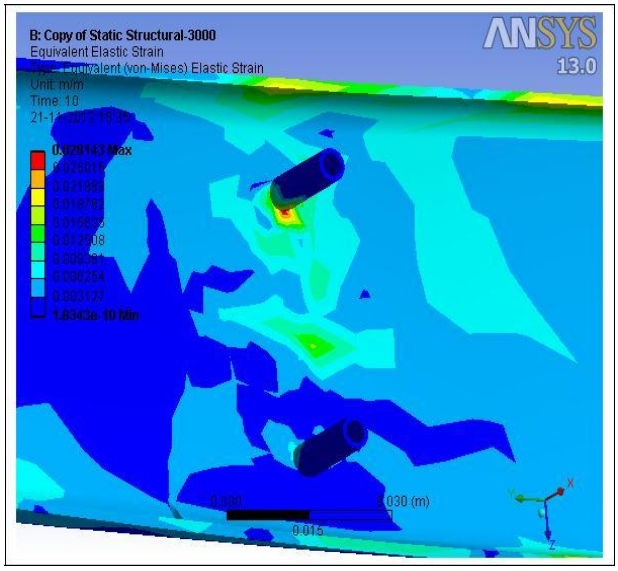

Figure 1.20: Von-Misses strain distribution – PP+EPDM

4. Findings:

The results obtained from the numerical simulation performed with ANSYS were compared and analysed for all the 3 reference materials. The important conclusions drawn from the simulation results are as follows;

- The structural deformation results obtained from the FE analysis clearly shows the maximum value for the Original Material and minimum value for PP+EPDM.
- The stress and strain distribution results confirm the minimum value for the material PP+EPDM.
- The Von-Misses stress distribution results obtained from the FE analysis shows that the maximum stresses are around the strain tensors.
- All the deformation and stress and strain distribution results are non-symmetric.
- The results show that the internal geometries of the strain tensors have no significant influence on the results and one can ignore these geometries in order to simplify the model.

B. Simulations results for crack propagation Analysis:

After developing a FE model for the crack propagation and fatigue strength analysis, the simulations are performed in ANSYS13. After performing the simulation in ANSYS for a 2000N ramped load the results are obtained in the form of deformations and stress distributions. The results obtained from ANSYS are described as follows;

1. Static Structural Results:

a. Stress Strain Relation: Figure 1.21 shows relation between Vonmises strain and Vonmises stress for three different materials for a 4000N ramped load. The results clearly show the lowest value for PP+EPDM, making it a clear favourite than the other two materials.

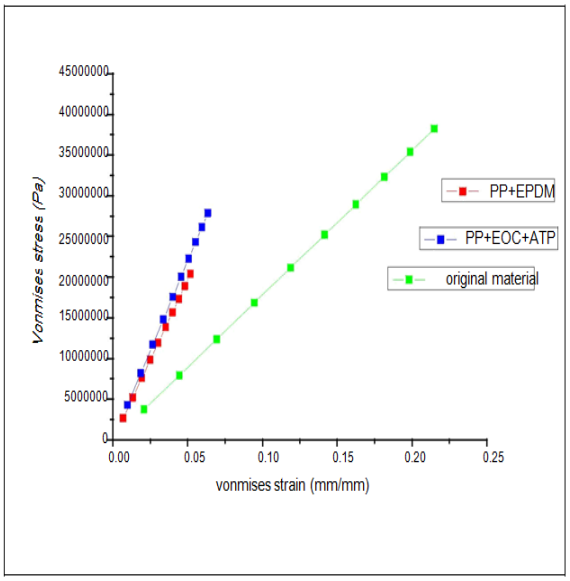

Figure 1.21. Vonmises Strain Vs Vonmises Stress

b. Stiffness Energy over Displacement: Figure 1.22 shows the effect of displacement on stiffness energy for three different materials for a 4000N ramped load. The results clearly show the lowest value for PP+EPDM.

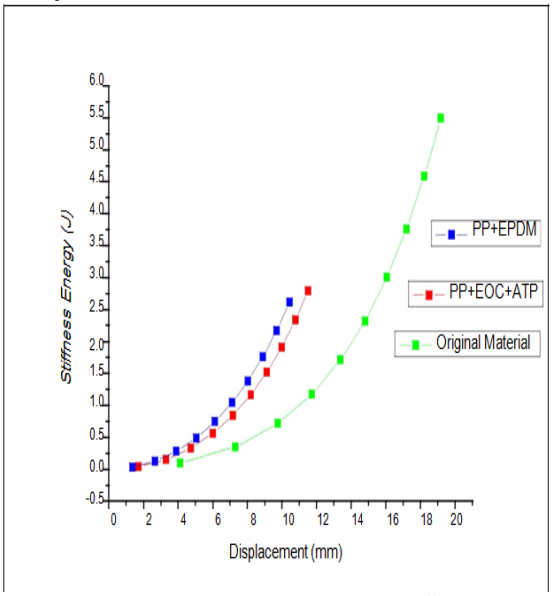

Figure 1.22 Displacement Vs Stiffness

2. Energy calculations: The area under the force-displacement curve is classically termed as strain energy. For each radius of the notch, a 4000N ramp load was applied along the 1 s step time. This means that the step time parameter (ranging from 0 to 1) allows determining for each increment of the applied load.

Therefore, the whole force-displacement curve was deduced (discredited using the step-time parameter) [11], for one single load case, by using the results for each increment.

Thus, the post-treating of the FEA gave for each load level the associated total displacement. An integration of the force-displacement curve (Figure 1.23) was performed, giving a strain energy–displacement curve (Figure 1.24).

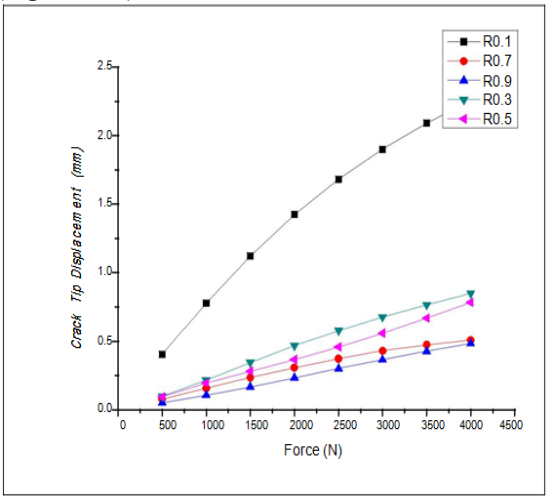

(a) Original Material

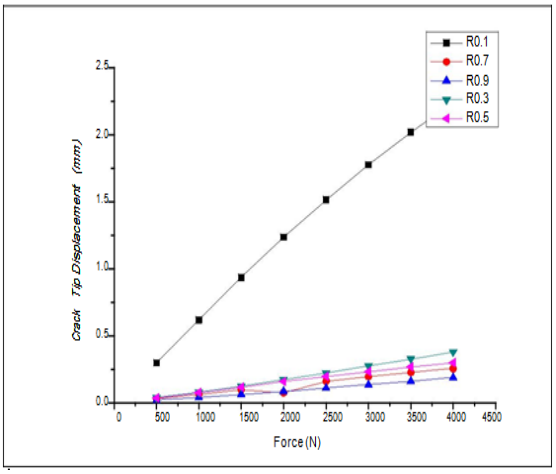

(b) PP+EOC+ATP

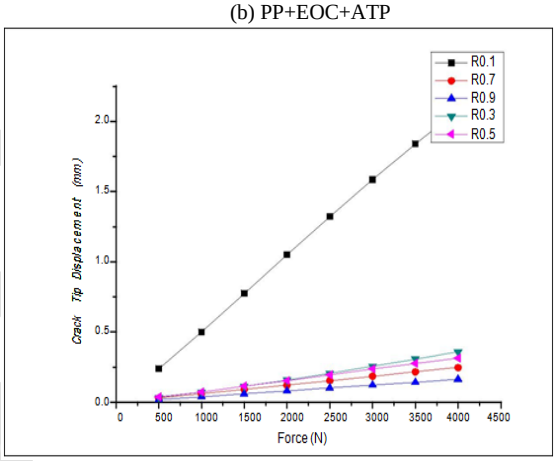

(c) PP+EPDM

Figure 1.23 Comparison of static structural test results of the different notched specimens

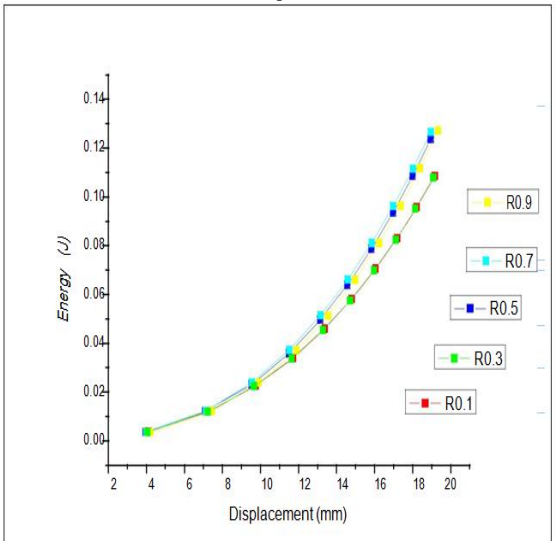

(a) Original Material

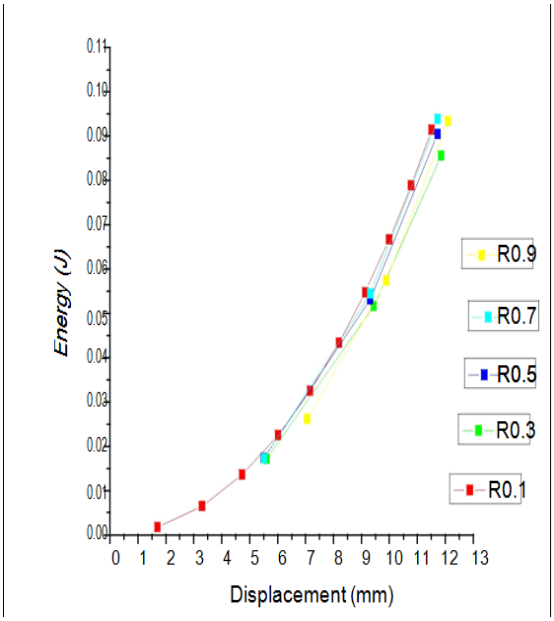

(b)PP+EOC+ATP

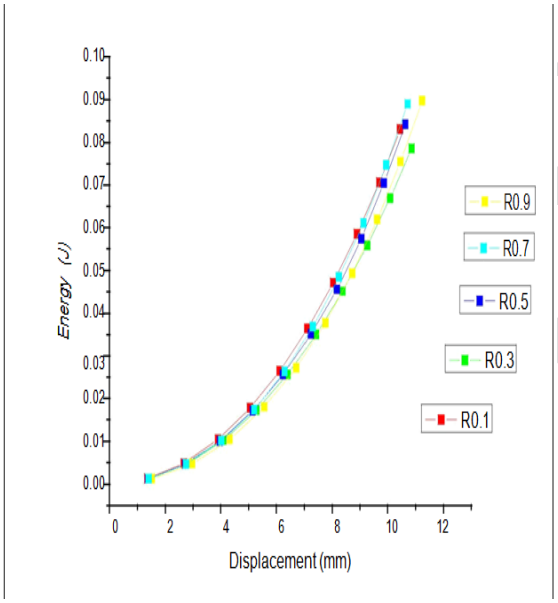

(c) PP+EPDM

Figure 1.24. Evolution of the tearing energy depending on the displacement for different notched specimens.

3. Crack Propagation and Stress Intensity: As per Figure 1.25, it shows the initiation and propagation of crack from the notch tip according to the time intervals, as there is the 4000N ramped loading for intervals across 0-1 sec. For the same ramped intervals it shows the stress intensities. Thus enables to see the variation in Stress Intensity with reference to Crack Length propagation.

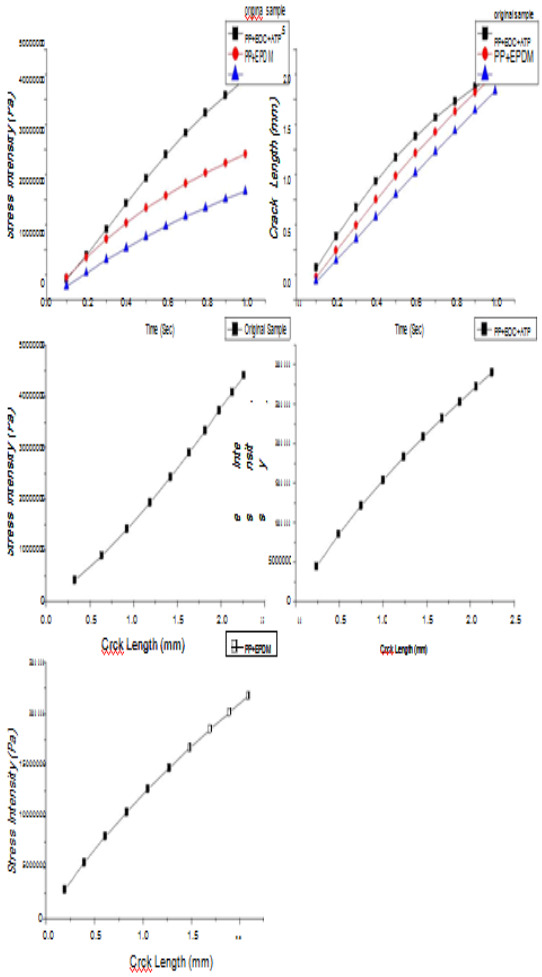

Figure 1.25 Variation of Stress Intensity Vs Crack Length

a. Crack Length Propagation along the Ramped intervals: Figure 1.26 (a) shows the crack length propagation along the ramped intervals for three different materials. Among which the original material shows the highest crack length propagation value and the material PP+EPDM shows the lowest crack length propagation value, as the graph shows. The reason is the predominant amount of PP the thermoplastic hard component in the blend, produced increased tensile strength, modulus and hardness [28].

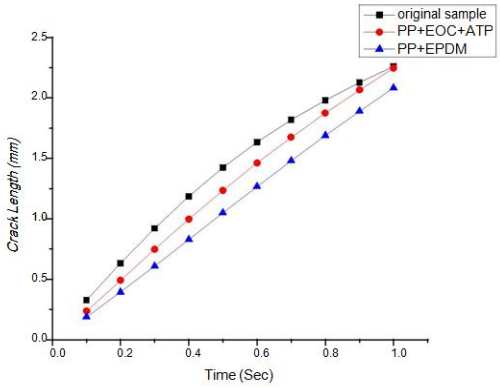

Figure 1.26 -(a) Time Vs Crack Length

b. stress intensity along the ramped intervals: Figure 1.26 (b) shows the variation in stress intensity along the ramped intervals for three different materials. Among which the original material shows the highest variation of stress intensity and the material PP+EPDM shows the lowest variation of stress intensity, as the graph shows. The reason is again the predominant amount of PP the thermoplastic hard component in the blend, produced increased tensile strength, modulus and hardness [28].

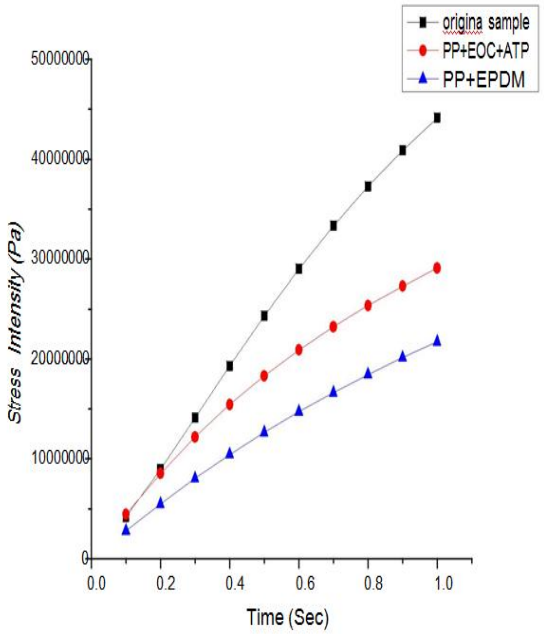

Figure 1.26 -(b) Time Vs Stress Intensity

c. Crack Length and Stress Intensity: - Figure 1.27 shows the variation in stress intensity along the ramped intervals with reference to crack length propagation for all three materials. It shows that for a maximum crack length growth of 2.084mm the corresponding stress intensity is 21724000Pa for PP+EPDM , which is the lowest among all the three different materials tested. Again the reason is the predominant amount of PP the thermoplastic hard component in the blend, produced increased tensile strength, modulus and hardness [28].

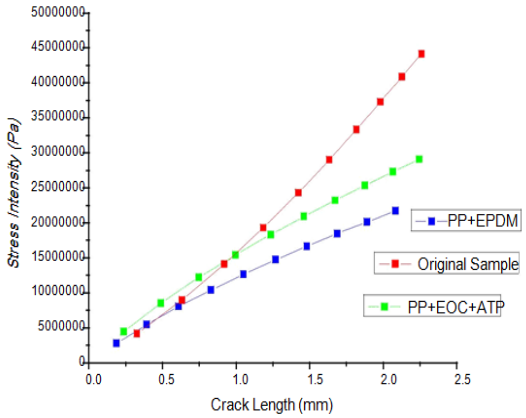

Figure 1.27 Crack Length Vs Stress Intensity

4. Effect of Notch size on crack propagation:

The simulation results are obtained in the form of maximum stress intensity and crack propagation rate. As expected, it has been found that the value of maximum stress intensity decreases with an increase in the notch radius. The maximum stress intensity of 44.1 MPa is found in the FE model with notch radius of 0.1 mm for the original product material. In order to understand the effect of notch size on the CG, simulations are performed until the notch radius reaches a value of 0.9 mm in all three cases. Table-2 summarizes the results obtained from the FE simulations performed. Finally, stress intensity is plotted as a function of crack length for all three cases in Figure 1.28 (a), Figure-1.28 (b) and Figure-1.28 (c) demonstrates the effect of notch radius on the CP.

Notch Radius (mm)	Maximum Stress Intensity (MPa)			Maximum Crack propagation (mm)		
	Original product material	PP+EOC+ATP	PP+EPDM	Original product material	PP+EOC+ATP	PP+EPDM
0.1	44.1	43	29.4	2.2608	2.2455	2.084
0.3	37	29.1	24.3	0.84794	0.37941	0.35905
0.5	29	24.7	22.5	0.7822	0.30025	0.31422
0.7	27.8	23.2	21.7	0.50872	0.25732	0.24828
0.9	26	21.8	18.4	0.48361	0.19037	0.1647

TABLE-2

The simulation results showed that the value of maximum stress intensity and the crack growth rate both decreases with an increase in the notch radius as shown in Figure-1.28 (a), Figure-1.28 (b), Figure-1.28 (c) for the original material of the product, PP+EOC+ATP and PP+EPDM respectively as shown in the graph. Hence, the crack growth rate increases with the sharper notch as expected.

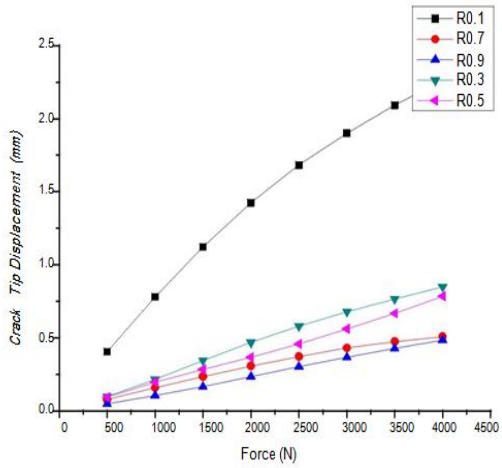

Figure 1.28 (a) for original product material

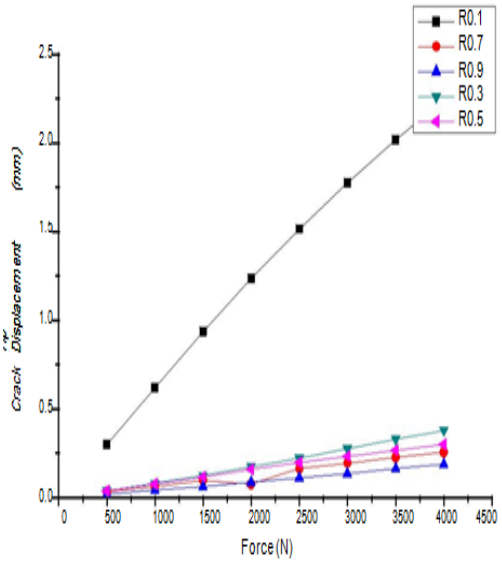

Figure 1.28 (b) for PP+EOC+ATP

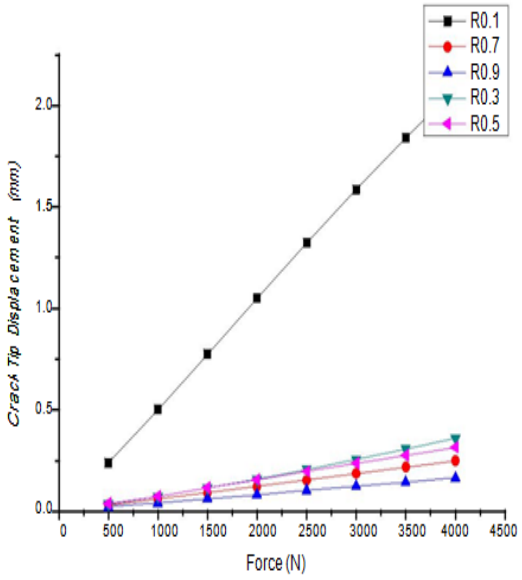

Figure 1.28 (c) for PP+EPDM

CONCLUSIONS:

The purpose of this project was to study the structural stability and crack propagation behaviour of the bumper protector structure based on FEA. The FEA is done with ANSYS13. An important aspect of this research was to compare the results from FEA for the three reference materials for five different Notch radius. The success in this manner depends both on the evaluation methods of the experiments and accuracy of FE models used in FEA. The crack propagation and static structural analysis is done with ANSYS13. A detailed study concerning different FE models with different geometries based on symmetry assumptions under static loading conditions were performed.

The simulation results obtained from the FE analysis performed with ANSYS showed the maximum deformations are found near the strain tensor. An important conclusion from these results is that the internal geometries of the stain tensors have no significant influence on the simulation results and one can ignore these geometries in order to simplify the FE model. In the light of this conclusion it is recommended to use simplified model without internal geometries of the strain tensors because these internal geometries sometimes also create problems during meshing due to the shape of these internal geometries.

REFFERENCES:

1. Mechanical and Fracture Behaviors of Elastomer-RichThermoplastic Polyolefin/SiCp Nanocomposites Cheng Zhu Liao and Sie Chin Tjong *Department of Physics and Materials Science, City University of Hong Kong, Tat Chee Avenue, Kowloon, Hong Kong* Correspondence should be addressed to Sie Chin Tjong, aptjong@cityu.edu.hk Received 3 November 2009; Accepted 10 April 2010
2. S. C. Tjong and Y. H. Ruan, "Fracture behavior of thermoplastic polyolefin/clay nanocomposites," *Journal of Applied Polymer Science*, vol. 110, no. 2, pp. 864–871, 2008.
3. J. K. Mishra, K.-J. Hwang, and C.-S. Ha, "Preparation, mechanical and rheological properties of a thermoplastic polyolefin (TPO)/organoclay nanocomposite with reference to the effect of maleic anhydride modified polypropylene as a compatibilizer," *Polymer*, vol. 46, no. 6, pp. 1995–2002, 2005.
4. L. P. Pook N. E. Frost and K. Matsh. Metal Fatigue. Oxford University Press, 1974.
5. ASTM: E1150/87 standard definitions of terms relating to fatigue. American Society for testing and Materials, (1987), pp. 1–10.
6. K.J. Miller., A historical perspective of the important parameter of metal fatigue; and problems for the next century. In: X.R. Wu and Z.G. Wang, Editors, Proceedings of the seventh international fatigue congress. Fatigue'99, Beijing 99, Higher Education Press EMAS (1999), pp. 15–39.
7. Y. Murakami, S. Harada, T. Endo, H. Tani-ishi and Y. Fukushima., Correlations among growth law of small cracks, low-cycle fatigue law and applicability of Miner's rule, Eng Fract Mech, 18 (1983) (5), pp. 909–924.
8. Stephens, Ralph I., Metal Fatigue in Engineering (Second edition ed.). John Wiley & Sons, Inc. 2001, pp. 69
9. Callister, W. D., Material Science and Engineering an Introduction, John Wiley & Sons, Inc. 2000.
10. Finite element analysis of dynamic crack propagation using remeshing technique A.R. Shahani *, M.R. Amini Fasakhodi

11. A comparative study on the damage initiation mechanism of elastomeric composites.
T. Da Silva Botelho*, N. Isac, E. Bayraktar School of Mechanical and Manufacturing Engineering, Supmeca/LISMMA-Paris, EA 2336, St-Ouen, France
12. O. Vardar., Effect of single OL in FCP. Engineering Fracture Mechanics, V-30, n-3 (1988), pp. 329-335.
13. J. J. Coner Julie A. Bannantine and J. Hand Rock., Fundamentals of metal fatigue analysis. Printice Hall, 1990
14. Sanford, R. J., 2003, Principles of Fracture Mechanics, Prentice Hall, Upper Saddle River, NJ
15. Sih, G. C., Some Basic Problems in Fracture Mechanics and New Concepts, Eng. Fracture Mech., Vol. 5 (1973), pp. 365-377
16. Atkinson, B.K., Fracture Mechanics of Rock, pp. 534, Academic Press, London UK, 1987. Chapter 1, 2, 4.
17. Anderson T.L., Fracture Mechanics Fundamentals and Applications, Second Edition, Taylor and Francis Ltd, Boca Raton, Florida, 1995, pp. 31-90, 566-598, 627-631
18. Dahlberg T. and Ekberg A., Failure Fracture Fatigue an Introduction, First Edition, Studentlitteratur, Sverige, 2002, pp. 63-205
19. Anderson, T.L., Fracture Mechanics: Fundamentals and Applications (CRC Press, Boston 1995)
20. Cook R.D., Malkus D.S., Plesha M.E. and Witt R.J., Concepts and Application of Finite Element Analysis, Fourth Edition, John Wiley and Sons Ltd, New York, 2001, pp. 202-219, 283-286
21. Sato,T., and Shimada,H., Evaluation of fatigue crack initiation life from a notch, Int. journal fatigue, Vol. 10, No. 4 Oct. 1988, PP. 243-247
22. Linear and Non Linear Analysis of Central Crack Propagation in Polyurethane Material - A Comparison Mubashir Gulzar
23. Stress Analysis, Crack Propagation and Stress Intensity Factor Computation of a Ti-6Al-4V Aerospace Bracket using ANSYS and FRANC3D By Priscilla L. Chin
24. Ashwell, D. G., and R. H. Gallagher, Editors, Finite Elements for Thin Shells and Curved Members, John Wiley and Sons, London, 1976
25. Madenci, E., and Guven, I., 2006, The Finite Element Application in Engineering using ANSYS®, Springer
26. Fracture study of modified TiO_2 reinforced PP/EPDM composite: mechanical behavior and effect of compatibilization Bishnu P. Panda, Smita Mohanty, Sanjay K. Nayak, Sushmita Pandit
27. Dynamically vulcanized PP/EPDM thermoplastic elastomers: Exploring novel routes for crosslinking with peroxides
Kinsuk Naskar Ph.D. Thesis, University of Twente, Enschede, The Netherlands 2004 ISBN 90 365 2045 2
28. Spur Gear Crack Propagation Path Analysis Using Finite Element Method Ananda Kumar Eriki, Member, IAENG, Ravichandra R, Member, IAENG and Mohd.Edilan Mustaffa.